SHORT PERIOD ACOUSTIC HEATING THEORY AND ITS APPLICATION TO THE CONSTRUCTION OF MODEL CHROMOSPHERES

P. ULMSCHNEIDER
Astronomisches Institut der Universität, Würzburg, G.F.R.

1 - Hydrodynamic equations

For a general introduction to the hydrodynamic equations and to sound waves, read the first few chapters of the excellent books of LANDAU and LIFSHITZ (1959) and ZELDOVICH and RAIZER (1966). STEIN and LEIBACHER (1974) give an up to date review of waves in the solar atmosphere. The articles of LISTER (1960) and HOSKIN (1964) show in greater detail the numerical methods used in this work.

Assume:		
	neutral, ideal gas	no viscosity
	plane geometry	no thermal conduction
	purely vertical motion	solar gravity

Let x be the outward geometrical distance (Euler coordinate). Consider a plate of gas at time $t = 0$ (see fig. 1).
The height x at time $t = 0$ is called Lagrange coordinate, a.

$$a \equiv x \quad \text{at} \quad t = 0 . \tag{1}$$

The plate has the thickness da and extends to infinity in y, z directions.
At a later time $t = t$ the plate, defined by a and da has moved to

$$x = x(a, t), \tag{2}$$

and has nof the thickness $\mathrm{d}x|_t$.
Conservation of mass requires for the mass density ρ:

$$\rho(a, t)\,\mathrm{d}x|_t = \rho(a, t = 0)\,\mathrm{d}a \equiv \rho_0(a)\,\mathrm{d}a . \tag{3}$$

Thus the specific volume v may be written

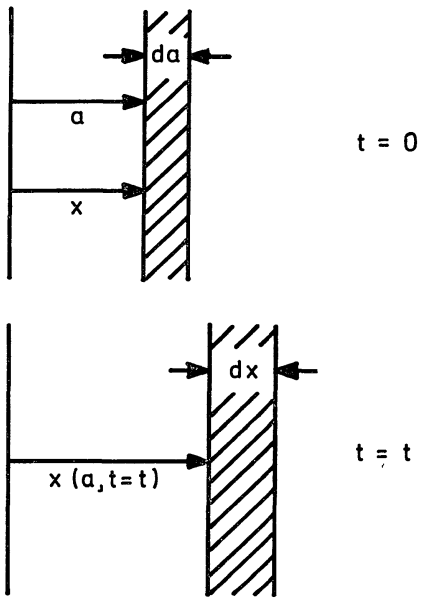

FIG. 1
Euler x and Lagrange a position of a plate of gas at time $t = 0$ and t.

$$v \equiv \left(\frac{\partial x}{\partial a}\right)_t = \frac{\rho_0}{\rho} . \tag{4}$$

The gas velocity u is defined as the temporal derivative of the position x of the plate,

$$u \equiv \left(\frac{\partial x}{\partial t}\right)_a . \tag{5}$$

Any change in density arises from a differential motion of the two faces of the plate,

$$\frac{1}{\rho}\left(\frac{\partial \rho}{\partial t}\right)_a = -\left(\frac{\partial u}{\partial x}\right)_t = -\frac{\rho}{\rho_0}\left(\frac{\partial u}{\partial a}\right)_t . \tag{6}$$

Considering action of pressure, p, and gravitational forces on the plate, the equation of motion is given by

$$\left(\frac{\partial u}{\partial t}\right)_a + \frac{1}{\rho_0}\left(\frac{\partial p}{\partial a}\right)_t + g = 0 \tag{7}$$

where g is gravitational acceleration at the solar surface. Because the entropy S is conserved in absence of radiation, the energy equation may be written as

$$\left(\frac{\partial S}{\partial t}\right)_a = \left.\frac{\mathrm{d}S}{\mathrm{d}t}\right|_{Rad} \tag{8}$$

where the right hand side is the radiative damping function which is usually given as a function of temperature T and ρ. For an ideal gas the equation of state is given by

$$p = \rho \frac{RT}{\mu} \tag{9}$$

where $\mu = 1.3$ g/Mol is the mean molecular weight and R the gas constant. The combined second and third law of thermodynamics connect S with p, ρ and T.

$$\left.\mathrm{d}S\right|_a = \frac{\left.\frac{1}{\gamma-1}\frac{R}{\mu}\mathrm{d}T\right|_a + p\,\mathrm{d}\left.\frac{1}{\rho}\right|_a}{T} = \left.\frac{1}{\gamma-1}\frac{R}{\mu}\frac{\mathrm{d}T}{T}\right|_a - \left.\frac{R}{\mu}\frac{\mathrm{d}\rho}{\rho}\right|_a . \tag{10}$$

Here $\gamma = 5/3$ is the ratio of specific heats. Sound velocity and scale height are given by

$$c^2 \equiv \gamma \frac{RT}{\mu} = \gamma \frac{p}{\rho} \tag{11}$$

and

$$H \equiv \frac{RT}{\mu g} . \tag{12}$$

2 - Adiabatic, linear waves in an isothermal gravitational atmosphere

Assume: static atmosphere $u = u_0 = 0$ (13)

isothermal atmosphere $T = T_0 = \text{const.}$ (14)

We have from eqs (7), (9) independent of t

$$\frac{\mathrm{d}p_0}{\mathrm{d}a} = -\rho_0 g \tag{15}$$

$$\rho_0 = \frac{\mu p_0}{RT} . \tag{16}$$

From this the density ρ_0 and pressure p_0 distributions are easily computed. Assume now small adiabatic disturbances in the static atmosphere,

$$\left.\frac{dS}{dt}\right|_{Rad} = 0 \tag{17}$$

$$\rho = \rho_0 + \rho', \quad p = p_0 + p', \quad u = u_0 + u' \quad \text{etc.} \tag{18}$$

and neglect quantities of second order.
From eqs (6), (13) we find

$$\frac{1}{\rho_0}\left(\frac{\partial \rho'}{\partial t}\right)_a + \left(\frac{\partial u'}{\partial a}\right)_t = 0\,. \tag{19}$$

Eliminating T from eq. (10) using (9), (11), (17) we have

$$dp'|_a = c^2\, d\rho'|_a\,. \tag{20}$$

Linearizing eq. (20) and integrating, using $\rho' = 0$ at $p' = 0$ we have

$$p' = c_0^2\, \rho'\,. \tag{21}$$

With this eq. (7) becomes

$$\left(\frac{\partial u'}{\partial t}\right)_a + \frac{c_0^2}{\rho_0}\left(\frac{\partial \rho'}{\partial a}\right)_t + \frac{1}{\rho_0}\left(\frac{\partial p_0}{\partial a}\right)_t + g = 0\,. \tag{22}$$

The last two terms cancel because of eq. (15).
Note that further differentiation of eqs (19), (22) and combining the results gives wave equations for u', ρ' or p' describing sound waves. We assume normal modes

$$\begin{aligned} u' &= A\, U\, e^{i(\omega t - Ka)} \\ \rho' &= A\, \rho_0\, \mathcal{R}\, e^{i(\omega t - Ka)} \\ K &= \kappa + ib\,. \end{aligned} \tag{23}$$

Here U, $\mathcal{R}$ are polarization factors, A an arbitrary amplitude with the absolute value much less than one and K a complex propagation vector.
With this we have from eqs (19) and (22)

$$\begin{bmatrix} i\omega & -i\kappa + b \\ -i\kappa c_0^2 + b c_0^2 - \dfrac{c_0^2}{H_0} & i\omega \end{bmatrix} \begin{bmatrix} \mathcal{R} \\ U \end{bmatrix} = 0 \tag{24}$$

where we have used

$$\left(\frac{\partial \rho_0}{\partial a}\right)_t = -\frac{\rho_0}{H_0} \tag{25}$$

which is derived from eq. (16) using (15), (12).
Defining the acoustic cut off frequency

$$\omega_A \equiv \frac{2\pi}{P_A} = \frac{c_0}{2H_0} \equiv \frac{\gamma g}{2 c_0} \tag{26}$$

eq. (24) has a non-trivial solution only if

$$b = \frac{\omega_A}{c_0} \tag{27}$$

and

$$\omega^2 - \omega_A^2 = \kappa^2 c_0^2 . \tag{28}$$

By inspection we find for the polarization factors

$$\mathcal{R} = \sqrt{1 - \left(\frac{\omega_A}{\omega}\right)^2} + i\frac{\omega_A}{\omega} \tag{29}$$

$$U = c_0 . \tag{30}$$

The complete solution is given by

$$u = A c_0 e^{\frac{\omega_A a}{c_0}} e^{i\left(\omega t - \frac{a}{c_0}\sqrt{\omega^2 - \omega_A^2}\right)} \tag{31}$$

$$\rho' = A \rho_0 \left[\sqrt{1 - \left(\frac{\omega_A}{\omega}\right)^2} + i\frac{\omega_A}{\omega}\right] e^{\frac{\omega_A a}{c_0}} e^{i\left(\omega t - \frac{a}{c_0}\sqrt{\omega^2 - \omega_A^2}\right)} \tag{32}$$

$$p' = c_0^2 \rho' . \tag{33}$$

From eqs (31) to (33) the phase shift between the u and ρ' oscillation is

$$\alpha = \arctan \frac{\frac{\omega_A}{\omega}}{\sqrt{1 - \left(\frac{\omega_A}{\omega}\right)^2}} . \tag{34}$$

For $\omega \gg \omega_A$ we have no phase shift, $\alpha = 0$, and the acoustic flux (Eckart, 1960 p. 52)

$$F_M = \frac{\int_{Period} p' u \, dt}{\int_{Period} dt} = \frac{\int_{Period} \rho_0 u^2 c_0 \, dt}{\int_{Period} dt} \cos \alpha . \qquad (35)$$

For $\omega \rightarrow \omega_A$ the phase shift $\alpha \rightarrow \frac{\pi}{2}$ and $F_M \rightarrow 0$. For $\omega \leq \omega_A$, as seen from eqs (29), (30), α is always $\frac{\pi}{2}$ and $F_M = 0$. Note that because of eqs (17), (21), (8) to (10) the phase shift between u and ρ' is the same as between u and p' and between u and T'.

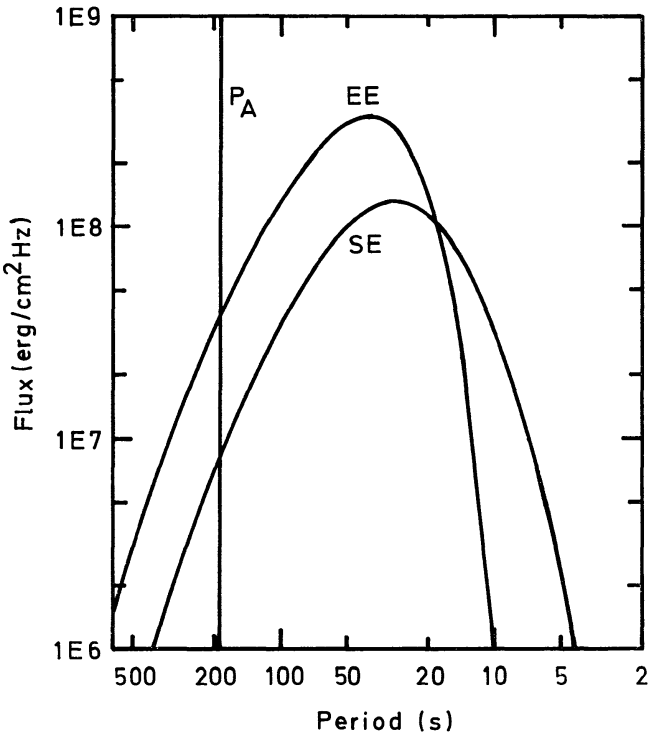

FIG. 2
STEIN's (1968) flux spectra. The vertical line marks the cut off period P_A at the temperature minimum.

In fig. 2 the frequency spectrum of acoustic waves in the solar atmosphere, generated by the turbulent motions in the convection zone is shown (STEIN 1968). The acoustic cut off period $P_A = 193$ s at the temperature minimum is indicated.

It is seen that the largest part of the spectrum is at periods small compared to P_A. This is the reason why these waves are called *short period oscillations.*

3 - Nonlinear isentropic waves, method of characteristics

Assume $g = 0$

$S = S_0 = const.$

It is convenient to choose for the two thermodynamic variables the entropy S (which in the present case is constant everywhere) and the sound velocity c. In order to eliminate ρ and p from eqs (6), (7) we solve eq. (10) for ρ and use (9), (11)

$$d\rho = \rho\left(\frac{2}{\gamma - 1}\frac{dc}{c} - \frac{\mu}{R}dS\right) \tag{36}$$

$$dp = \rho\left(\frac{2c}{\gamma - 1}dc - \frac{c^2 u}{\gamma R}dS\right) \tag{37}$$

under the assumption of constant S and $g = 0$ using eqs (36), (37) in (6) and (7) we have

$$\frac{3}{c}\left(\frac{\partial c}{\partial t}\right)_a + \frac{\rho}{\rho_0}\left(\frac{\partial u}{\partial a}\right)_t = 0 \tag{38}$$

$$\left(\frac{\partial u}{\partial t}\right)_a + \frac{3\rho c}{\rho_0}\left(\frac{\partial c}{\partial a}\right)_t = 0\,. \tag{39}$$

With eq. (36) and $S = $ const. we find

$$\frac{\rho}{\rho_0} = \frac{1}{v} = \left(\frac{c}{c_0}\right)^3. \tag{40}$$

Adding eq. (38)$\cdot c$ to (39) we have

$$\left(\frac{\partial u}{\partial t} + \frac{c^4}{c_0^3}\frac{\partial u}{\partial a}\right) + 3\left(\frac{\partial c}{\partial t} + \frac{c^4}{c_0^3}\frac{\partial c}{\partial a}\right) = 0\,. \tag{41}$$

Consider a function $f(a, t)$. For a change of f along a given curve $a(t)$ we have

$$df = \frac{\partial f}{\partial t}dt + \frac{\partial f}{\partial a}da = \frac{\partial f}{\partial t}dt + \frac{\partial f}{\partial a}\frac{da}{dt}dt$$

or: (42)

$$\left.\frac{df}{dt}\right|_{\text{along } a(t)} = \frac{\partial f}{\partial t} + \frac{\partial f}{\partial a}\frac{da}{dt}\,.$$

Thus from eq. (41) with (42) we find:

$$\mathrm{d}u + 3\,\mathrm{d}c = \mathrm{d}(u + 3c) = 0 \tag{43}$$

along

$$\frac{\mathrm{d}a}{\mathrm{d}t} = \frac{c^4}{c_0^3} \tag{44}$$

where the curve described by eq. (44) is called C^+ characteristic.
Similarily, subtracting eq. (38)$|\cdot c$ from (39) we find

$$\mathrm{d}u - 3\,\mathrm{d}c = \mathrm{d}(u - 3c) = 0 \tag{45}$$

along

$$\frac{\mathrm{d}a}{\mathrm{d}t} = -\frac{c^4}{c_0^3} \tag{46}$$

the C^- characteristic.

With these equations we have for the Riemann invariants J^+, J^-

$$J^+ \equiv u + 3c = const. \text{ along } C^+ \tag{47}$$

$$J^- \equiv u - 3c = const. \text{ along } C^- . \tag{48}$$

The physical significance of the characteristics can ben elucidated by going over to the Euler (Laboratory) frame by using eqs (44), (46), (4), (40)

$$\frac{\mathrm{d}x^\pm}{\mathrm{d}t} = \frac{\mathrm{d}a^\pm}{\mathrm{d}t}\left(\frac{\partial x}{\partial a}\right)_t + u = u \pm c . \tag{49}$$

Thus the characteristics are world lines of disturbances traveling with sound velocity $\pm c$ relative to a medium that is moving with u.

Assume that the solution is given everywhere on the a axis between the points A and B. (see (fig. 3).

We thus know at

$$A: \; u_A, c_A \quad \text{or} \quad J^+, J^-(A)$$

$$B: \; u_B, c_B \quad \text{or} \quad J^+, J^-(B)$$

We want to compute the solution at point P. We have from eqs (47), (48)

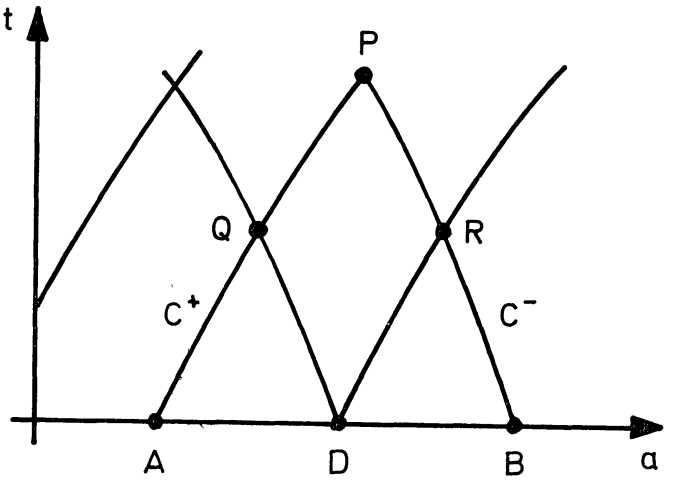

FIG. 3
Domain of dependence.

$$J^+(P) = J^+(A) \; : \; u_P + 3\,c_P = u_A + 3\,c_A \tag{50}$$

$$J^-(P) = J^-(B) \; : \; u_P - 3\,c_P = u_B - 3\,c_B\,. \tag{51}$$

This system (50), (51) can be solved for u_P and c_P

$$u_P = \frac{u_A + u_B + 3\,c_A - 3\,c_B}{2} = \frac{J^+(A) + J^-(B)}{2} \tag{52}$$

$$c_P = \frac{3\,c_A + 3\,c_B + u_A - u_B}{6} = \frac{J^+(A) - J^-(B)}{6}\,. \tag{53}$$

The slope of the C^+, C^- characteristics at P is then

$$\left.\frac{\mathrm{d}\,a}{\mathrm{d}\,t}\right|_P^{\pm} = \pm\frac{{c_P}^4}{{c_0}^3}\,. \tag{54}$$

We know now u_P and c_P but we do not know the position a_P, t_P of P. This position may be found approximately by triangulation using the known slopes of the characteristics (45), (46) at A, B. A better position of P can be found by first computing the solution and position of points Q and R using values at A, D and D, B and then computing P etc. From this limiting process it is obvious that the *solution vector* (u_P, c_P, a_P, t_P) at P is completely determined by the initial conditions on the segment $A\,B$ of the a axis and is independent of the initial values outside this segment. The triangle $A\;B\;P$ is called the *domain of dependence.*

Consider in fig. 4 the gas bounded by a piston.

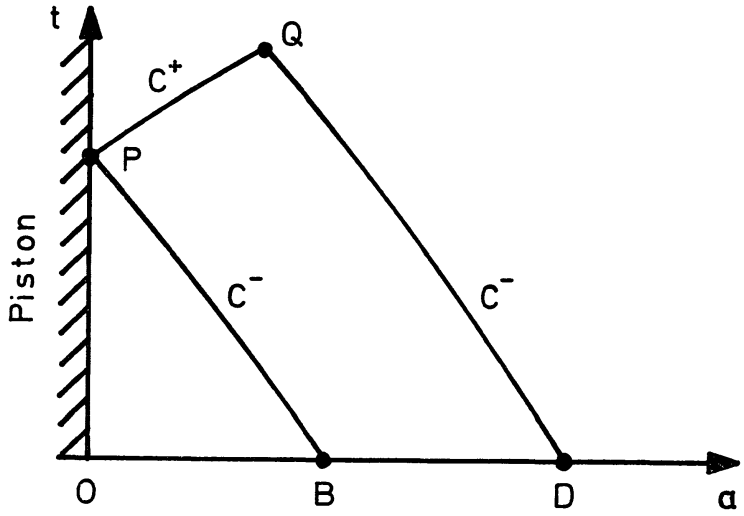

FIG. 4
Piston boundary.

At point P the velocity u is a prescribed function of t

$$u_P = U_{Pist}(a = 0, t) . \tag{55}$$

The Lagrange position of the piston is $a = 0$.
We have

$$J^-(P) = J^-(B) : U_{Pist}(a = 0, t_P) - 3 c_P = u_B - 3 c_B . \tag{56}$$

Here c_P could be computed if t_P were known. But t_P can be determined approximately using the slope $\left.\frac{da}{dt}\right|_B^-$.
The complete knowledge of the initial values at the segment OB determines the solution vector at P uniquely.
Eventually the solution vector at Q can be determined using

$$J^+(Q) = J^+(P) \quad \text{and} \quad J^-(Q) = J^-(D) . \tag{57}$$

This procedure to advance the solution vector in time using approximate positions a, t triangulated with straight lines is called *method of characteristics.*

4 - Simple waves

Simple waves are waves for which $J^-(a, t) = \text{const.}$

$$J^-(a, t) = u(a, t) - 3\,c(a, t) \equiv \text{const.} \tag{58}$$

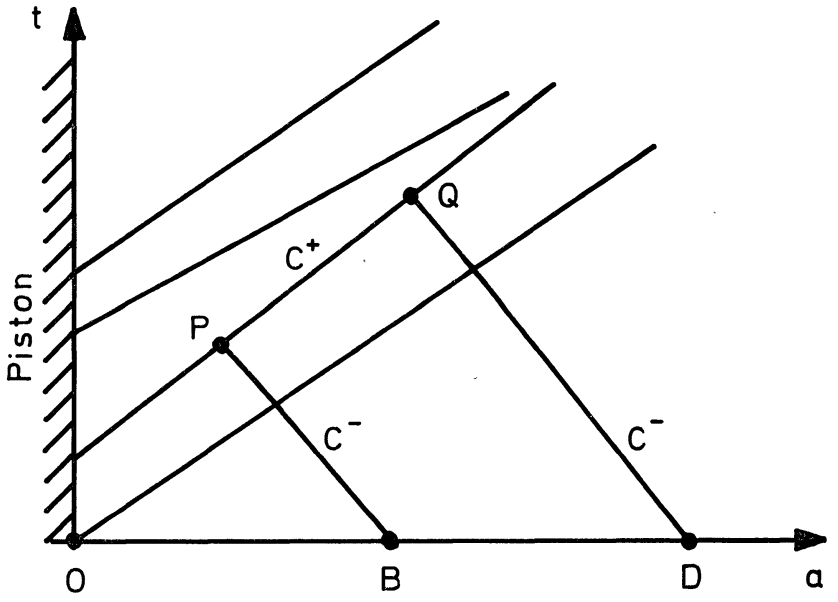

FIG. 5
Simple wave generated by piston motion.

Usually one has such waves when a disturbance from a piston travels into an undisturbed nongravitational isothermal atmosphere. Because the disturbance (see fig. 5) starts for $t = 0$ at $a = 0$, we have at every point of the a-axis at $t = 0$ that

$$J^-(a, t = 0) = -3\,c_0 = \text{const.} \tag{59}$$

Consider fig. 5. Because $J^+ = \text{const.}$ along $C^+ : \overline{PQ}$ and because $J^-(P) = J^-(B) = J^-(D) = J^-(Q) = \text{const.}$ after eq. (59) we have $c_P = c_Q = \text{const.}$ and $u_P = u_Q = \text{const.}$ after (52), (53) and thus $\dfrac{da^+}{dt} = \text{const.}$ after eq. (54).

In a simple wave the C^+ *characteristics are straight lines, and the values of* c *and* u *are conserved along these* C^+ *characteristics.*

This property of simple waves can be exploited to construct the development of the wave profile.

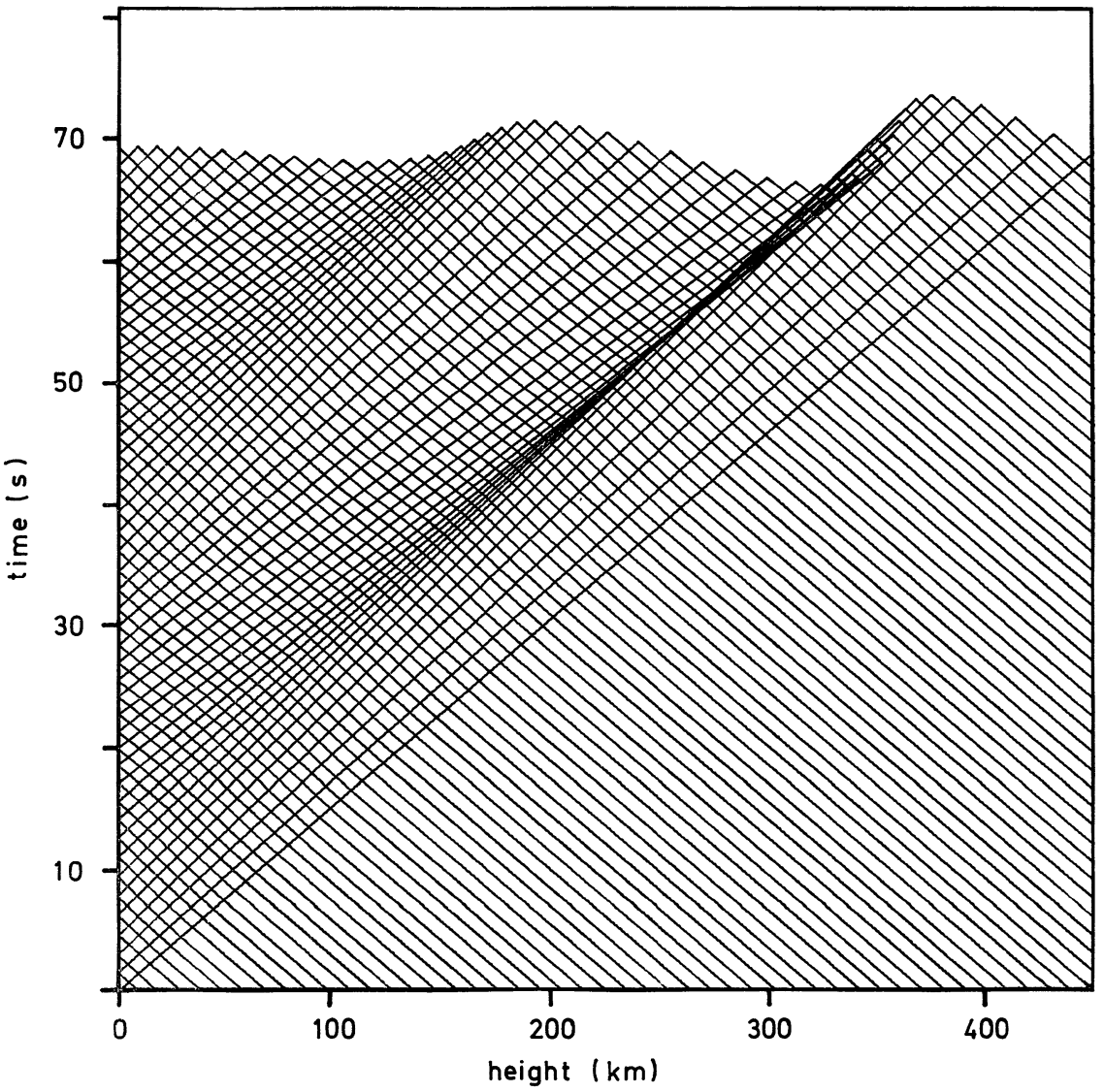

FIG. 6
Field of characteristics in a homogeneous atmosphere which is excited by a piston.

Fig. 6 shows an isentropic calculation. Here the isothermal atmosphere is excited by a piston starting at time $t = 0$. We have

$$u_{Pist} = -u_0 \sin \frac{2\pi}{P} t \tag{60}$$

where $u_0 = 1/10\, c_0$, the period $P = 30$ s and the temperature $T_0 = 4000$ °K. It is seen that a simple wave results with the C^+ characteristics being straight lines.

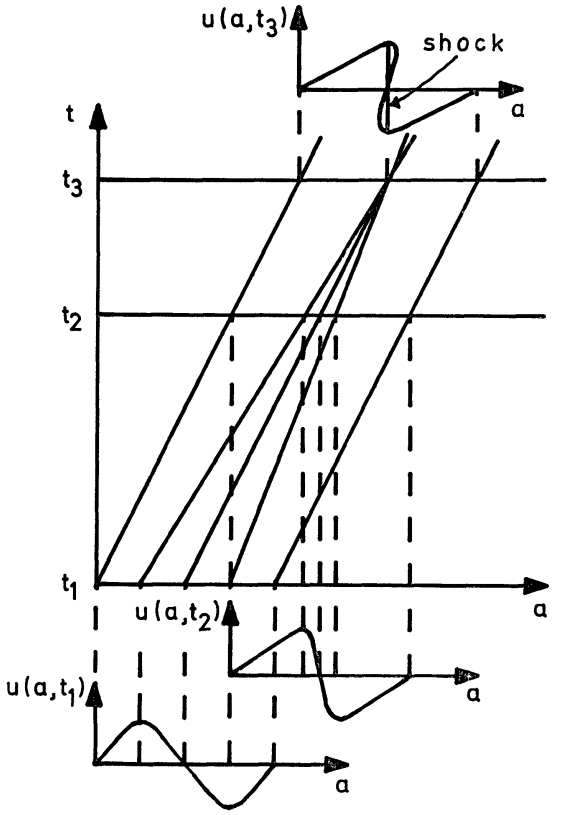

FIG. 7
Development of the wave profile in a simple wave.

5 - Shocks

Fig. 6 shows that after some time C^+ characteristics intersect and form shocks. Using the properties of simple waves this behavior is explained in fig. 7. The conservation of the velocity amplitudes along C^+ leads to a wave distortion and to multivalued profiles after the C^+ intersect. The shock discontinuity replaces the multivalued profile. This allows a geometric construction of the shock and a calculation of the dissipation of the wave energy by the shock (see Section 11).

6 - Nonlinear nonadiabatic waves in non isothermal gravitational atmospheres

Using eqs (36) and (37) to eliminate the derivatives of ρ and p from eqs (6) and (7) we have with (4)

$$\frac{2}{\gamma - 1}\frac{\partial c}{\partial t} - \frac{\mu c}{R}\frac{\partial S}{\partial t} + \frac{c}{v}\frac{\partial u}{\partial a} = 0 \qquad (61)$$

and

$$\frac{\partial u}{\partial t} + \frac{2}{\gamma - 1} \frac{c}{v} \frac{\partial c}{\partial a} - \frac{\mu c}{\gamma R} \frac{c}{v} \frac{\partial S}{\partial a} + g = 0 . \tag{62}$$

Adding eqs (61) and (62) using (8) the ordinary differential equation

$$\mathrm{d}u + \frac{2}{\mu - 1} \mathrm{d}c - \frac{\mu c}{\gamma R} \left(\mathrm{d}S + (\gamma - 1) \left. \frac{\mathrm{d}S}{\mathrm{d}t} \right|_{Rad} \mathrm{d}t \right) + g \, \mathrm{d}t = 0 \tag{63}$$

is obtained along the C^+ characteristic given by

$$\frac{\mathrm{d}a}{\mathrm{d}t} = \frac{c}{v} \tag{64}$$

where v from eqs (4) and (36) is found to be

$$v = \left(\frac{c_0}{c} \right)^{\frac{2}{\gamma - 1}} e^{-\frac{(S - S_0)\mu}{R}} . \tag{65}$$

Here c_0 and S_0 are the sound velocity and entropy distributions of the static atmosphere.
Subtracting eq. (61) from (62) using (8) we find

$$\mathrm{d}u - \frac{2}{\gamma - 1} \mathrm{d}c + \frac{\mu c}{\gamma R} \left(\mathrm{d}S + (\mu - 1) \left. \frac{\mathrm{d}S}{\mathrm{d}t} \right|_{Rad} \mathrm{d}t \right) + g \, \mathrm{d}t = 0 \tag{66}$$

along the C^- characteristic, given by

$$\frac{\mathrm{d}a}{\mathrm{d}t} = -\frac{c}{v} \tag{67}$$

Finally from eq. (8) we have

$$\mathrm{d}S = \left. \frac{\mathrm{d}S}{\mathrm{d}t} \right|_{Rad} \mathrm{d}t \tag{68}$$

along the C^0 characteristic, a = const.

For an arbitrary temperature distribution the initial sound velocity c_0 is found using eq. (11). In a static atmosphere, $u_0 = 0$, the initial entropy distribution S_0 is found using eq. (62)

$$\frac{\mathrm{d}S_0}{\mathrm{d}a} = \frac{\gamma R}{\mu c_0} \left(\frac{2}{\gamma - 1} \frac{\mathrm{d}c_0}{\mathrm{d}a} + \frac{g}{c_0} \right) . \tag{69}$$

Note that the concept of conservation of the Riemann invariants eqs (43), (45) is now generalized into eqs (63), (66). The method of characteristics is generalized likewise, using now 3 characteristics. In fig. 8 the procedure to compute the unknown position and state at point P, where we have now the unknowns a, t, u, c, S, is as follows.

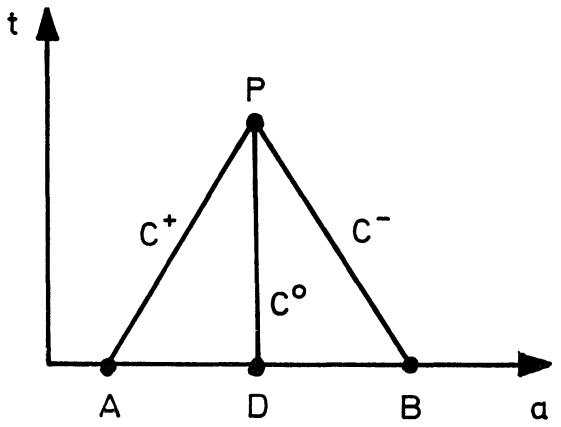

FIG. 8
Computation of the solution at point P using the three characteristics C^0, C^+, C^-.

With the known solution everywhere at $\overline{AB}$ the slopes of the C^+, C^- characteristics at A and B may be computed from eqs (64), (65), (67). Thus the position a, t of P may be found by triangulation. The position a_P determines the C^0 characteristic and therefore point D. With the known solution (entropy S and radiative damping function $\left.\frac{dS}{dt}\right|_{Rad}$) at D, eq. (68) may be integrated to give the entropy S at P. The integration of eqs (63), (66) gives the remaining unknowns u_P and c_P at P. This procedure to compute the solution at P is quite similar to the one discussed in Section 3. Boundary points are treated therefore in a likewise manner.

Fig. 9 shows the result of a calculation of an adiabatic ($\left.\frac{dS}{dt}\right|_{Rad} = 0$) wave of period $P = 30$ s with $u_0 = 1/10\, c_0$ in eq. (60) taking an initial atmosphere of $T = 4000$ °K and solar gravity. It is seen that the C^+ characteristics, except in the nodes, are not straight lines anymore as in the isentropic case of fig. 6.

The increasing density amplitude (see eq. (32)) in a gravitational atmosphere leads to an increasing sound velocity amplitude (eq. (36)) and to an increasing curvature (eqs (64), (65), (67)) of the characteristics. Fig. 10 shows the result of an adiabatic wave in an empirical atmospheric model (HSRA, GINGERICH et al.

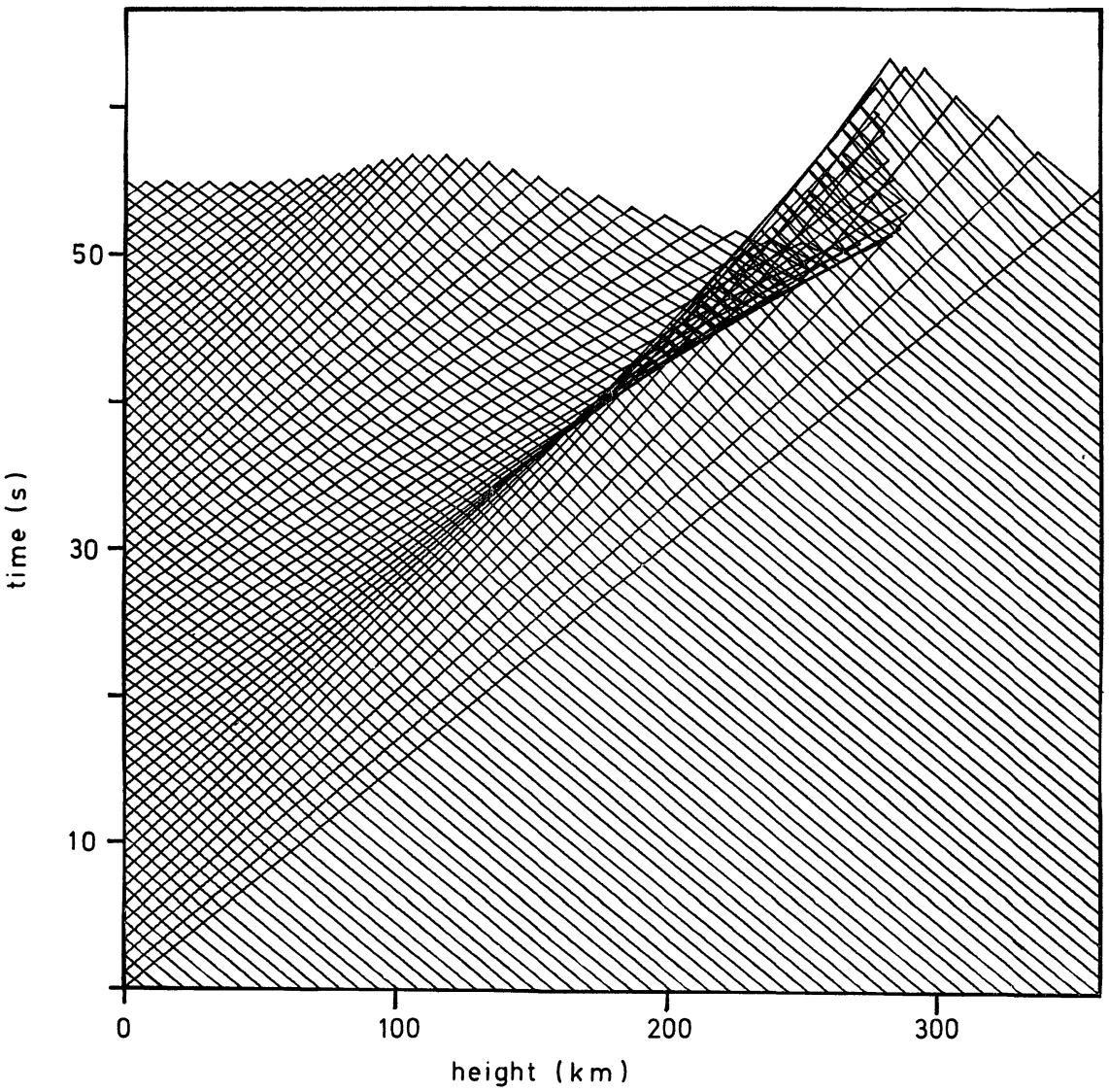

FIG. 9
Field of characteristics in an isothermal gravitational atmosphere which is excited by a piston.

1971). Here the period was $P = 30$ s and the velocity amplitude $u_0 = 1/10\ c_0$. The C^+ characteristics are now seen to be curved even in absence of a disturbance due to the decreasing sound velocity of the atmosphere (eqs (64), (65)). The heights of shock formation of waves with various periods and fluxes in the HSRA atmospheric model is seen in fig. 13. Because the rate of profile distortion is due to the rate of convergence of the C^+ characteristics and because this rate depends on the amplitude (eqs (64), (65)) waves of greater flux form shocks earlier. In

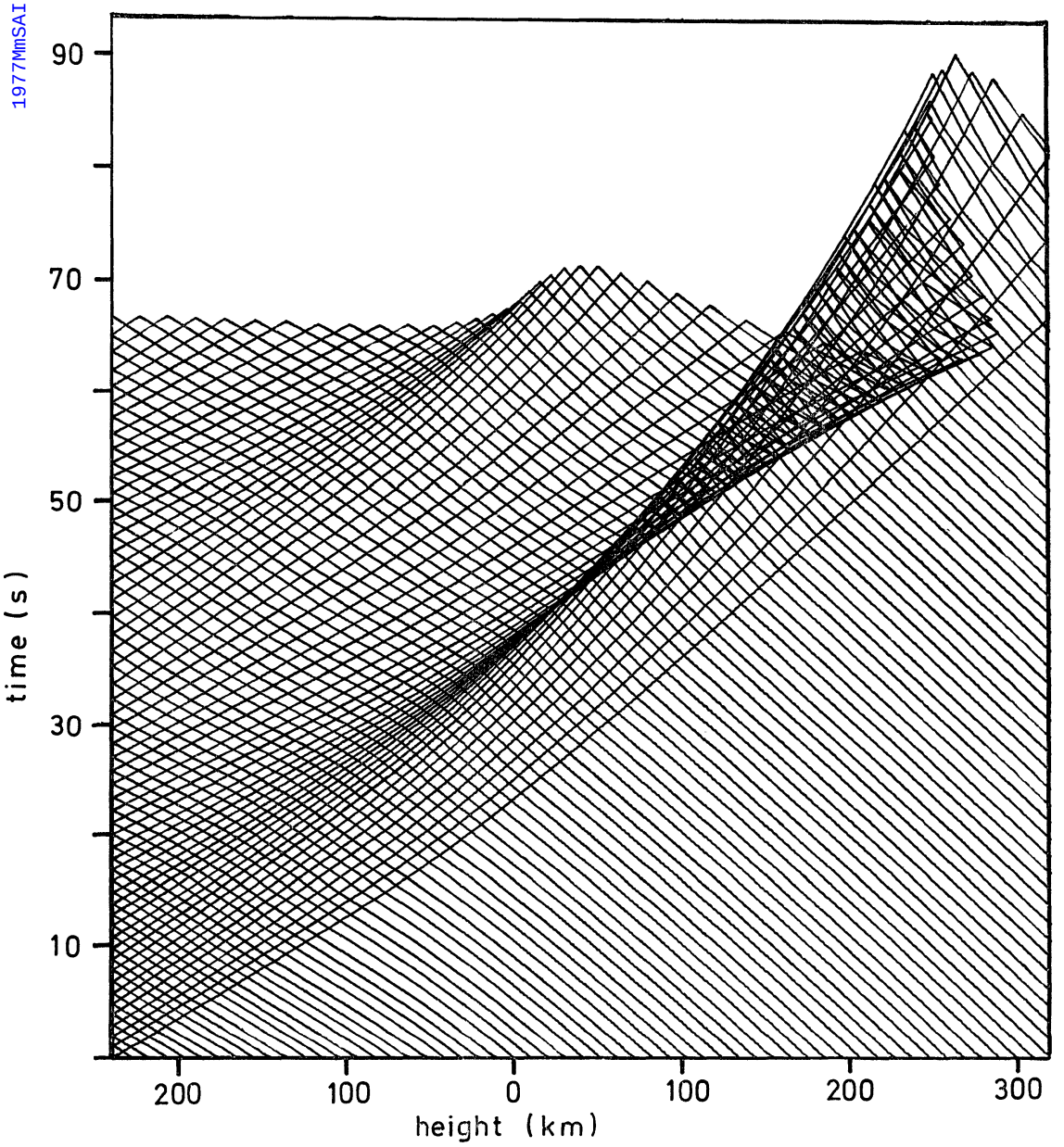

FIG. 10
Field of characteristics in the HSRA atmosphere which is excited by a piston.

waves having short periods the areas of strongly differing slope of the C^+ characteristics (the magnitude of the slope depends only on the flux of the wave) will be closely spaced, leading to an early intersection, that is to a low height of shock formation (KALKOFEN and ULMSCHNEIDER 1976).

7 - Radiative damping

Because radiative damping may decrease by an order of magnitude the acoustic energy that reaches the chromosphere, an accurate treatment of radiation is of great importance. Consider the transfer equation of radiation (MIHALAS 1971)

$$\mu \frac{\mathrm{d}I_\nu}{\mathrm{d}x} = -k_\nu (I_\nu - S_\nu) . \tag{70}$$

Here I_ν is the specific intensity, ν the frequency, μ the angle cosine, k_ν the absorption coefficient and S_ν the source function. As radiative damping of acoustic waves propagating radially out of the Sun happens mainly at optical depths $\tau_{5000} = 0.1$ to 10, departures from local thermal equilibrium (LTE) are unimportant thus

$$S_\nu = B_\nu \equiv \frac{2h\nu^3}{C_L^2} \frac{1}{e^{\frac{h\nu}{kT}} - 1} \tag{71}$$

where B_ν is the Planck function, h Planck's constant and C_L the velocity of light.

Integrating eq. (70) over angles and frequencies gives with eq. (71)

$$\frac{\mathrm{d}F_R}{\mathrm{d}x} = -4\pi \int_0^\infty k_\nu (J_\nu - B_\nu) \mathrm{d}\nu \tag{72}$$

where

$$F_R \equiv 2\pi \int_0^\infty \int_{-1}^{+1} \mu I_\nu \, \mathrm{d}\mu \, \mathrm{d}\nu \tag{73}$$

is the radiation flux and

$$J_\nu \equiv \frac{1}{2} \int_{-1}^{+1} I_\nu \, \mathrm{d}\mu \tag{74}$$

is the mean intensity.

Using eqs (70) and (71), I_ν can be computed for $\mu \geq 0$ using

$$I_\nu (\tau_\nu, \mu) = \int_{\tau_\nu}^{\tau_{\nu\mathrm{Max}}} B_\nu (T(\tau')) \, e^{-\frac{\tau' - \tau_\nu}{\mu}} \frac{\mathrm{d}\tau'}{\mu} + I_\nu^+ (\tau_{\nu\mathrm{Max}}, \mu) \, e^{-\frac{\tau_{\nu\mathrm{Max}} - \tau_\nu}{\mu}} \tag{75}$$

and for $\mu \leq 0$ using

$$I_\nu(\tau_\nu, \mu) = \int_{\tau_{\nu\mathrm{Min}}}^{\tau_\nu} B_\nu(T(\tau')) e^{-\frac{\tau_\nu - \tau'}{|\mu|}} \frac{\mathrm{d}\tau'}{|\mu|} + I_\nu^-(\tau_{\nu\mathrm{Min}}, \mu) e^{-\frac{\tau_\nu - \tau_{\nu\mathrm{Min}}}{|\mu|}} \tag{76}$$

where

$$\tau_\nu = -\int_0^x k_\nu \, \mathrm{d}x' \tag{77}$$

and $I_\nu^+(\tau_{\nu\mathrm{Max}}, \mu)$, $I_\nu^-(\tau_{\nu\mathrm{Min}}, \mu) = 0$ are boundary conditions. The entropy S lost by an outflux of photons is then given by

$$\left.\frac{\mathrm{d}S}{\mathrm{d}t}\right|_{Rad} = -\frac{1}{\rho T}\frac{\mathrm{d}F_R}{\mathrm{d}x} = \frac{4\pi}{\rho T}\int_0^\infty k_\nu (J_\nu - B_\nu)\,\mathrm{d}\nu\,. \tag{78}$$

At large optical depth $\tau_\nu \gg 1$ this equation may be approximated using the Eddington approximation

$$\left.\frac{\mathrm{d}S}{\mathrm{d}t}\right|_{Rad} = \frac{4\pi}{\rho T}\int_0^\infty \frac{1}{3} k_\nu \frac{\mathrm{d}^2 J_\nu}{\mathrm{d}\tau_\nu^2}\mathrm{d}\nu\,. \tag{79}$$

This is the *diffusion approximation*. At small optical depths $\tau_\nu \ll 1$ the mean intensity is practically the constant surface value $J_\nu(0)$ thus

$$\left.\frac{\mathrm{d}S}{\mathrm{d}t}\right|_{Rad} = \frac{4\pi}{\rho T}\int_0^\infty k_\nu (J_\nu(0) - B_\nu)\,\mathrm{d}\nu\,. \tag{80}$$

This is the *optically thin approximation.*

The procedure to compute this radiative damping function $\left.\frac{\mathrm{d}S}{\mathrm{d}t}\right|_{Rad}$ is as follows: Because radiation processes occur with the speed of light and the hydrodynamic processes with the speed of sound, radiation processes are essentially instantaneous compared to the hydrodynamic time scales. It is thus necessary to have the solution u, c, S at every height for a fixed time t. From the thermodynamic variables c, S we may compute T and ρ and thus B_ν and k_ν for every height and frequency point. Here k_ν must be taken from an opacity

table. Integrating eq. (77) we find τ_ν and integrating eqs (75) and (76) we find I_ν. The integrations of eqs (75) and (76) are performed recursively starting from the respective boundaries. In order to reproduce the diffusion and optically thin approximations the source function is evaluated using parabolic sections see fig. 11.

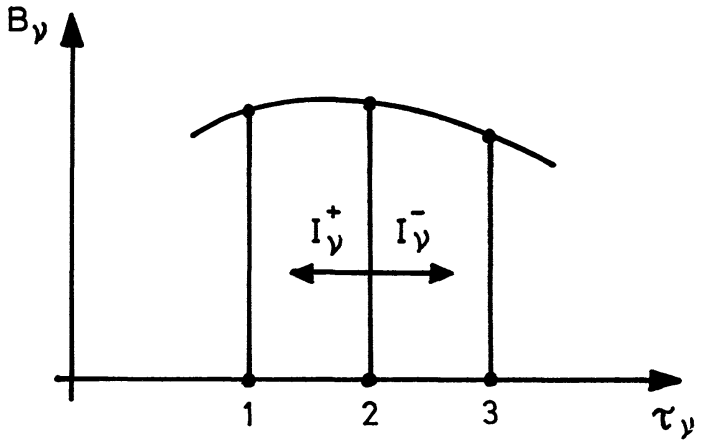

FIG. 11
Interpolation of the source function B between grid points.

Consider a parabola going through the source functions at points 1, 2, 3. The ingoing intensity I_ν^- at point 2 is evaluated using the segment 1-2 of this parabola and the outgoing intensity I_ν^+ is evaluated using the segment 23 of the same parabola. After evaluation of the specific intensities I_ν, the mean intensity J_ν is computed using eq. (74). Subsequent frequency integration (eq. (78)) gives the damping function (KALKOFEN and ULMSCHNEIDER 1976).

8 - Modified method of characteristics

We have seen in the previous section that for the inclusion of radiation the solution of the hydrodynamic equations must be given for every height, a, at the same time t. In the full method of characteristics the intersection points of the characteristics do not lie on $a\,t$ = const. line (see figs 6, 9, 10). In order to make certain that the intersection points lie all at the same time level $\overline{P\,Q}$, the method of characteristics is modified as shown in fig. 12.

Here the position a, t of the points Q, P etc. are predetermined. The characteristics intersecting at point P now emanate from the old time level at points R, S. The solution at R, S is interpolated from the known solution at the grid points A, D, B. Aside of this procedure the modified characteristic method proceeds like the full characteristic method.

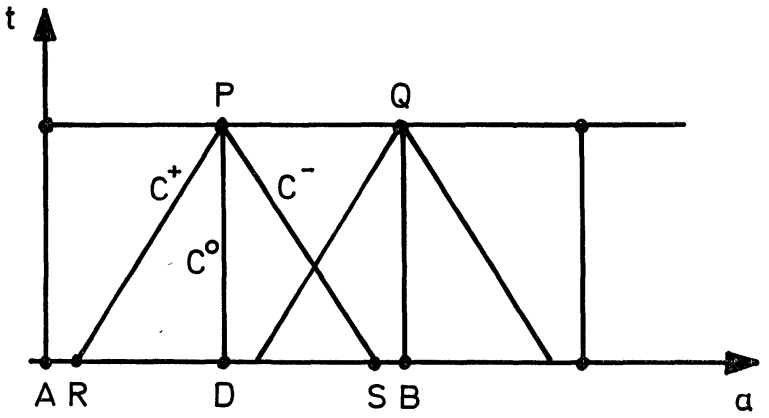

FIG. 12
Computation of the solution at point P in the modified method of characteristics.

9 - Perturbation method for nonlinear radiatively damped waves in gravitational atmospheres

With the specification of the radiative damping function $\left.\frac{dS}{dt}\right|_{Rad}$ in eq. (78) the eqs (63) to (68) can now be solved in principle with the modified characteristics method similar to the procedure outlined in Section 3. In practice the evaluation of eq. (78) needs a large number of frequency and angle points (more than 30 for a realistical photospheric model) and an opacity table including a large number of absorbers. In order to keep the computation time within reasonable limits we evaluated eq. (78) with one angle and one frequency point, employing the grey approximation for which an opacity table is given by KURUCZ (1970). With a one frequency and one angle point calculation a realistic model of the Sun can *not* be made. Thus we use a published nongrey model as static atmosphere on top of which the acoustic waves propagate (KALKOFEN and ULMSCHNEIDER 1976). For this model we have from eq. (72)

$$\frac{dF_R^0}{dx} = -4\pi \int_0^\infty k_\nu^0 (J_\nu^0 - B_\nu^0)\, d\nu . \tag{81}$$

In the perturbed atmosphere we have

$$\frac{dF_R^0}{dx} + \frac{dF_R^1}{dx} = -4\pi \int_0^\infty (k_\nu^0 + k_\nu^1)(J_\nu^0 + J_\nu^1 - B_\nu^0 - B_\nu^1)\, d\nu . \tag{82}$$

Here the quantities of first order are due to the wave.

Subtracting eq. (81) from (82) and neglecting quantities of second order we have

$$\frac{\mathrm{d}F_R^1}{\mathrm{d}x} = -4\pi \int_0^\infty k_\nu^0 (J_\nu^1 - \bar{S}_\nu^1)\,\mathrm{d}\nu \tag{83}$$

where J_ν^1 is computed using eqs (74), (75), (76) replacing B_ν by the angle dependent source function

$$S_\nu^1(\mu) = B_\nu^1 - \frac{k_\nu^1}{k_\nu^0}(I_\nu^0(\mu) - B_\nu^0) \tag{84}$$

and where

$$\bar{S}_\nu^1 = \frac{1}{2}\int_{-1}^{+1} S_\nu^1(\mu)\,\mathrm{d}\mu\,. \tag{85}$$

We use the grey approximation of eq. (83).

10 - Theoretical temperature minima

Using eqs (78), (83) for the description of radiative damping eqs (63) to (68) may now be solved with the modified method of characteristics. We follow the development of the wave until shock formation. Because the shock dissipates rapidly as soon as it forms we expect that the shock formation height is close to the height of the temperature minimum (T. M.).

In fig. 13 shock formation heights for waves of different period and initial fluxes are shown. It is seen that for waves of initial fluxes between 3 and $6 \cdot 10^7$ erg/cm^2 s and periods between 25 and 45 s the empirical T. M. can be reproduced.

These acoustic fluxes agree well with those computed from the Lighthill theory,

$$F_M = \int_0^\infty 38\,\frac{\rho\,\bar{v}^8}{\alpha\,c^5}\,\frac{\mathrm{d}x}{H} \tag{86}$$

where $\bar{v}$ is the mean turbulent velocity, α the ratio of mixing length/pressure scale height. Table 1 exhibits acoustic fluxes computed with eq. (86) using a stellar envelope program. In addition values of Stein (1968) are given, who uses more elaborate expressions in place of eq. (86). Note that values of $\alpha = 1.1$ to 1.3 are presently accepted for the Sun (Christiansen-Dalsgaard and Gough 1976).

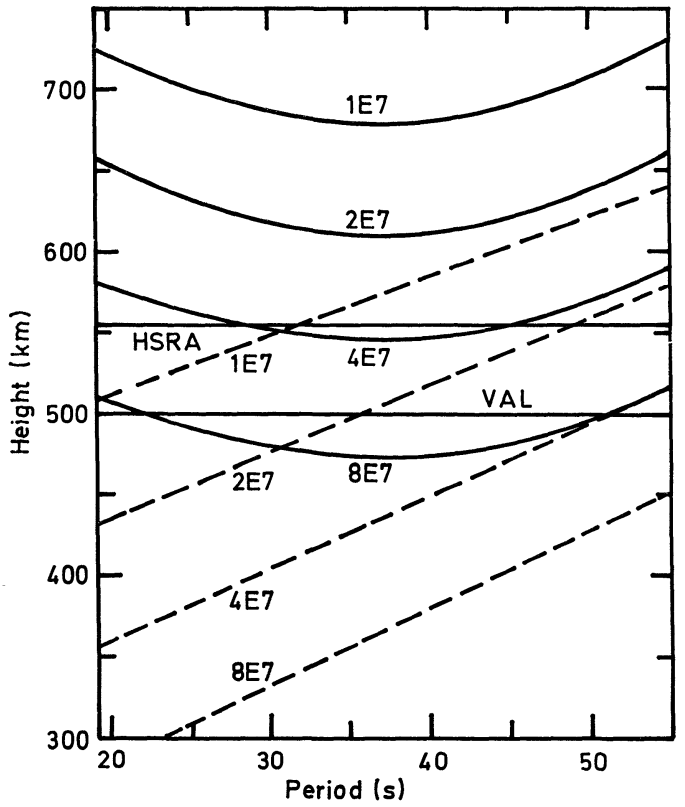

FIG. 13
Shock formation heights (drawn) in the HSRA atmosphere for waves of different period with the initial acoustic flux as parameter. Dashed lines indicate shock heights for adiabatic waves. HSRA and VAL show heights of the temperature minima in the HSRA and VAL models.

TABLE I - Theoretical and empirical temperature minima for the Sun.

α	Mode	F_M (erg/cm^2 s)	P_{Max} (s)	h_o (km)	F_o (erg/cm^2 s)
1.0	Eq. (86)	1.6 E7	27.5	650	3.2 E6
1.25		3.0 E7	26.0	590	5.0 E6
1.5		5.1 E7	24.5	540	7.2 E6
2.0		1.1 E8			
2.0	STEIN 1968, EE	9.9 E7	25		
2.0	STEIN 1968, SE	5.5 E7	40		
1.5	Stein EE Scaled	4.5 E7	25		
1.5	Stein EE Scaled	2.5 E7	40		
	empirical HSRA			550	5.0 E6
	empirical VAL			500	

The period of the waves agrees also well with theoretical expectations as seen in fig. 2 (STEIN 1968). Because of the v^{-8} dependence the main contribution to eq. (86) arises within $1/2\ H$ at the top of the convection zone. Thus the period is approximately

$$P_{Max} \approx \frac{P_A}{10} \approx \frac{H}{2\,\bar{v}} \approx \frac{120\ \text{km}}{2 \cdot 2\ \text{km/s}} = 30\ \text{s}\,. \tag{87}$$

Table 1 shows a comparison of the theoretical T. M. with two empirical T. M. for the Sun.

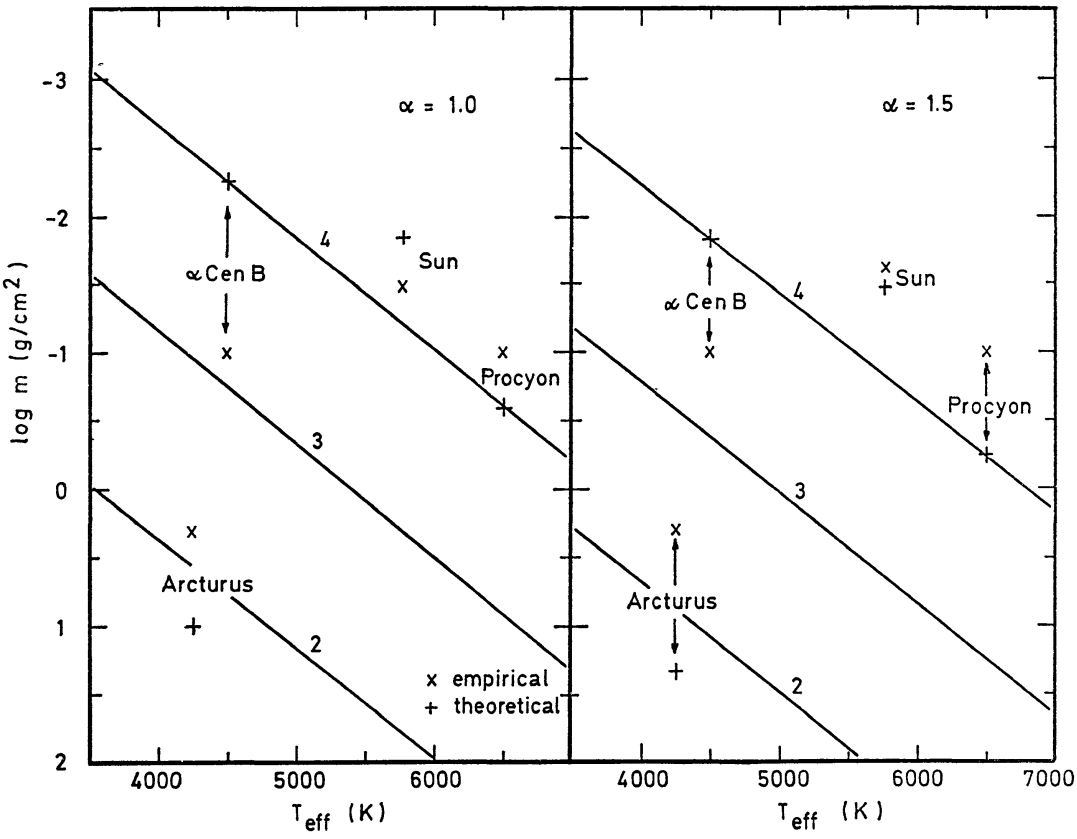

FIG. 14
Shock formation heights on a mass scale for various stars of different T_{eff} with log g as parameter. Crosses indicate special stars. α is the ratio of mixing length to pressure scale height.

Fig. 14 shows such a comparison for other stars where the empirical T.M. were taken from AYRES (1975). Another quantity of great importance is the acoustic flux F_0 at shock formation. This flux should heat the chromosphere and should therefore be comparable to the empirical chromospheric radiation flux. In fig. 15 the flux F_0 is shown as function of the wave period and the initial acoustic

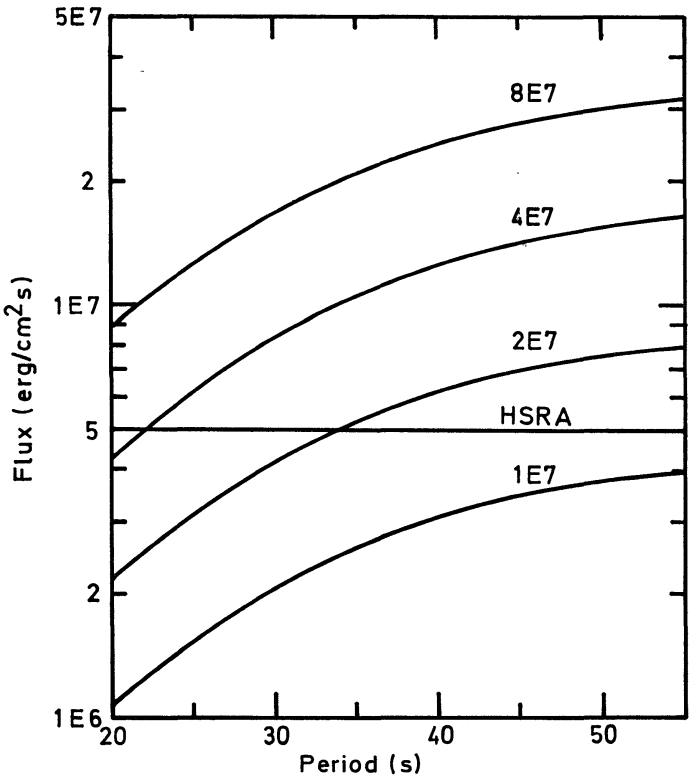

FIG. 15
Acoustic flux at the position of shock formation (drawn) in the HSRA as function of period with the initial acoustic flux as parameter. HSRA indicates chromospheric radiation flux.

flux. The empirical radiation flux is produced by waves which have initial flux between 1 and $5 \cdot 10^7$ erg/cm^2 s and periods less than 45 s. Table I shows a theoretical prediction for the Sun. Fig. 16 shows a comparison for other stars. Here the chromospheric fluxes are taken from AYRES (1975).

11 - Weak shock heating formulas for the chromosphere

The time-independent approach to construct model chromospheres starts usually by specifying heating formulas which describe the shock dissipation. Other heating mechanisms like conductive or viscous heating (MCWHIRTER et al. 1975) can be shown to be unimportant in the chromosphere (VANBEVEREN and DE LOORE 1976). A heating formula for weak shocks may be derived from the behaviour of simple waves exhibited in figs 5, 6, that the velocity amplitude u and the sound velocity c remain constant along a C^+ characteristic. This behaviour will be valid as long as the amplitudes are sufficiently small such that shock heating does not change the straight line nature of the C^+ behind the shock (see fig. 6).

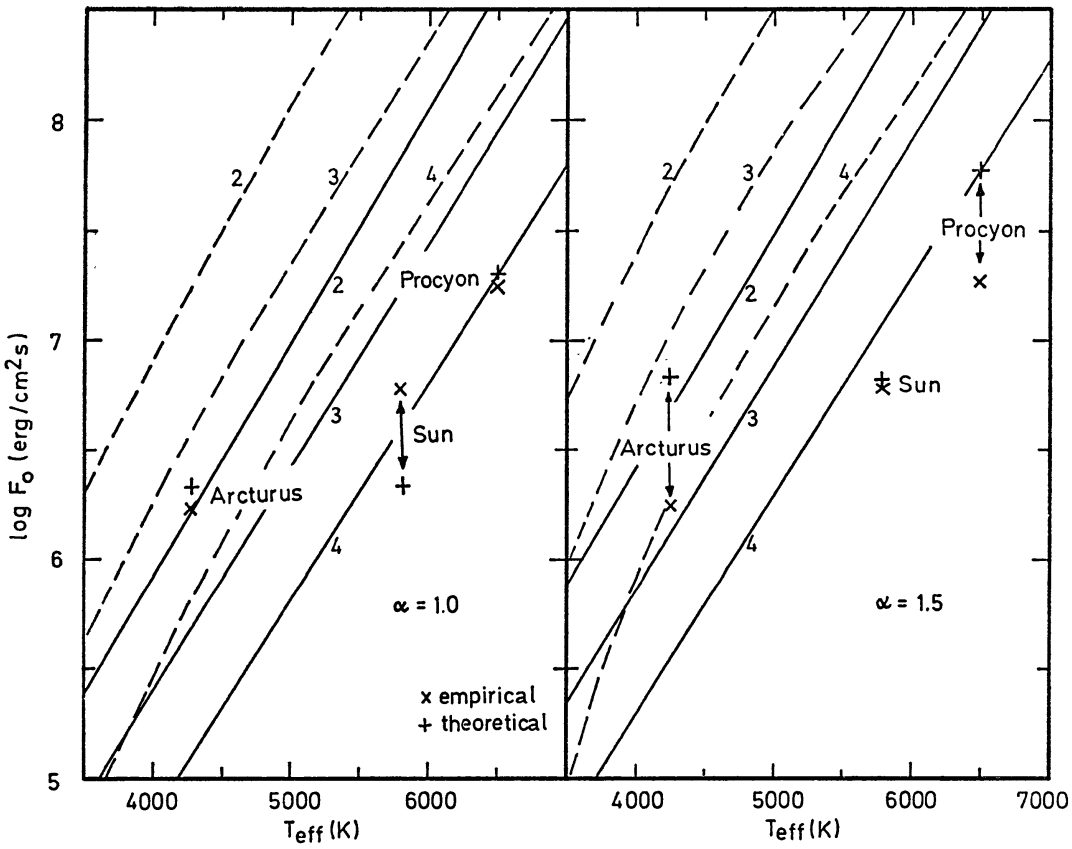

FIG. 16
Acoustic flux at shock formation (drawn) for various stars of different T_{eff} with log g as parameter. Crosses indicate special stars. Initial acoustic flux is shown dashed.

Consider a fully developed sawtooth type shock wave (fig. 17). From the definition of simple waves, eqs (58), (59) we have

$$c = c_0 + \frac{\gamma - 1}{2} u \,. \tag{88}$$

With this and the slope of the C^+ given by eq. (44), we are able to construct the development of the wave profile. As the heating formulas are usually given in the Euler frame we find using eqs (49), (88)

$$\left.\frac{\mathrm{d}x}{\mathrm{d}t}\right|^{+} = u + c = c_0 + \frac{\gamma + 1}{2} u \,. \tag{89}$$

Similarily to fig. 7 the development of the sawtooth wave may be constructed using eq. (89) as seen in fig. 17. The original wave OBAE at $t = 0$ with the discontinuity A B is seen to develop at $t = t$ into a multivalued profile OB'A'E.

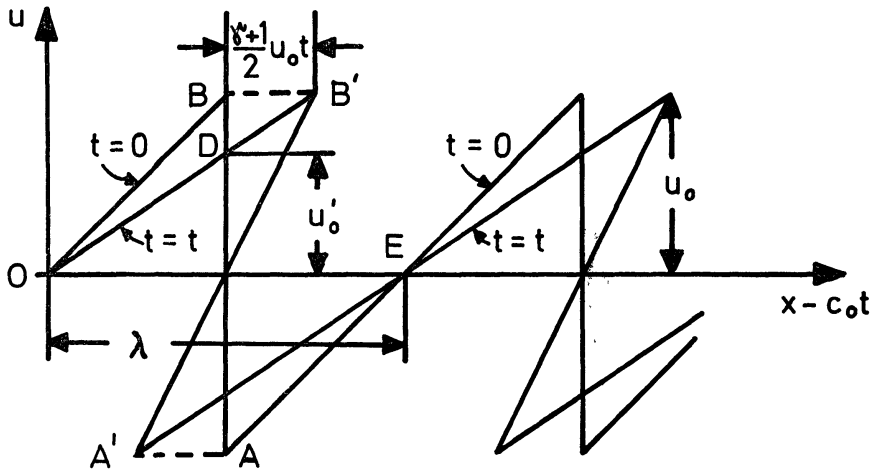

FIG. 17
Development of a sawtooth shock wave.

Actually only the profile ODCE is realized with the discontinuity DC. For short period waves the flux at $t = 0$ using eq. (35) and $\alpha = 0$ is

$$F_M = \frac{2}{\lambda}\int_0^{\frac{\lambda}{2}} \rho_0 c_0 u^2(x)\,dx \tag{90}$$

where λ is the wavelength. Taking

$$u(x) = \frac{2u_0}{\lambda}x \tag{91}$$

where u_0 is the velocity amplitude we find from eq. (90)

$$F_M = \frac{1}{3}\rho_0 c_0 u_0^2 . \tag{92}$$

At time t (see fig. 17) the velocity amplitude is reduced to u_0'

$$u_0' = \frac{u_0}{1 + (\gamma+1)u_0\frac{t}{\lambda}} . \tag{93}$$

Using $x = c_0 t$ in eq. (93) we find

$$F_M(x) = \frac{1}{3}\rho_0 c_0 u_0^2 \left(1 + (\gamma+1)\frac{u_0}{c_0}x\right)^{-2} \tag{94}$$

Differentiation with respect to x and using $\lambda = c_0 P$ gives at $t = 0$

$$\frac{dF_M}{dx} = -2(\gamma+1)\frac{u_0}{c_0^2 P}F_M \tag{95}$$

where P is the wave period. Eliminating u_0 from eq. (95) with eqs (92), (11) we find (ULMSCHNEIDER 1971a, KUPERUS 1965, BRAY and LOUGHEAD 1974)

$$\frac{dF_M}{dx} = -\left(\frac{12(\gamma+1)}{\gamma p_0 c_0^3}\right)^{1/2}\frac{1}{P}F_M^{3/2}. \tag{96}$$

Recently VANBEVEREN and DE LOORE (1976) have used a simplified version of eq. (95) assuming

$$2(\gamma+1)\frac{u_0}{c_0} \approx 1.4. \tag{97}$$

We see however no necessity for making such an approximation.

12 - Time independent models for the chromosphere

It can be shown that in the chromosphere at heights below 1600 km (above $\tau_{5000} = 1$) one may safely neglect wave pressure, thermal conduction, viscosity and the mass and energy flow due to the solar wind. For a time independent model one simply solves the hydrostatic and energy equations assuming the weak shock heating formula (96)

$$\frac{dp_0}{dx} = -\rho_0 g \tag{98}$$

$$\frac{dF_M}{dx} = -\left(\frac{12(\gamma+1)}{\gamma p_0 c_0^3}\right)^{1/2}\frac{1}{P}F_M^{3/2} \tag{99}$$

$$\frac{dF_M}{dx} + \frac{dF_R}{dx} = 0. \tag{100}$$

This system of equations together with eqs (9), (11) can be solved if boundary conditions p_0, F_{M0} at $x = x_0$ are given and the wave period P is specified, provided the radiative cooling function $\frac{dF_R}{dx}$ is given. Assuming that the radiation loss is primarily due to H^- we may write

$$\frac{dF_R}{dx} = 4\pi \int_0^\infty k_\nu^{H^-} (B_\nu(T) - B_\nu(T_B))\, d\nu \qquad (101)$$

where T_B is the boundary temperature for which the minimum temperature can be taken.

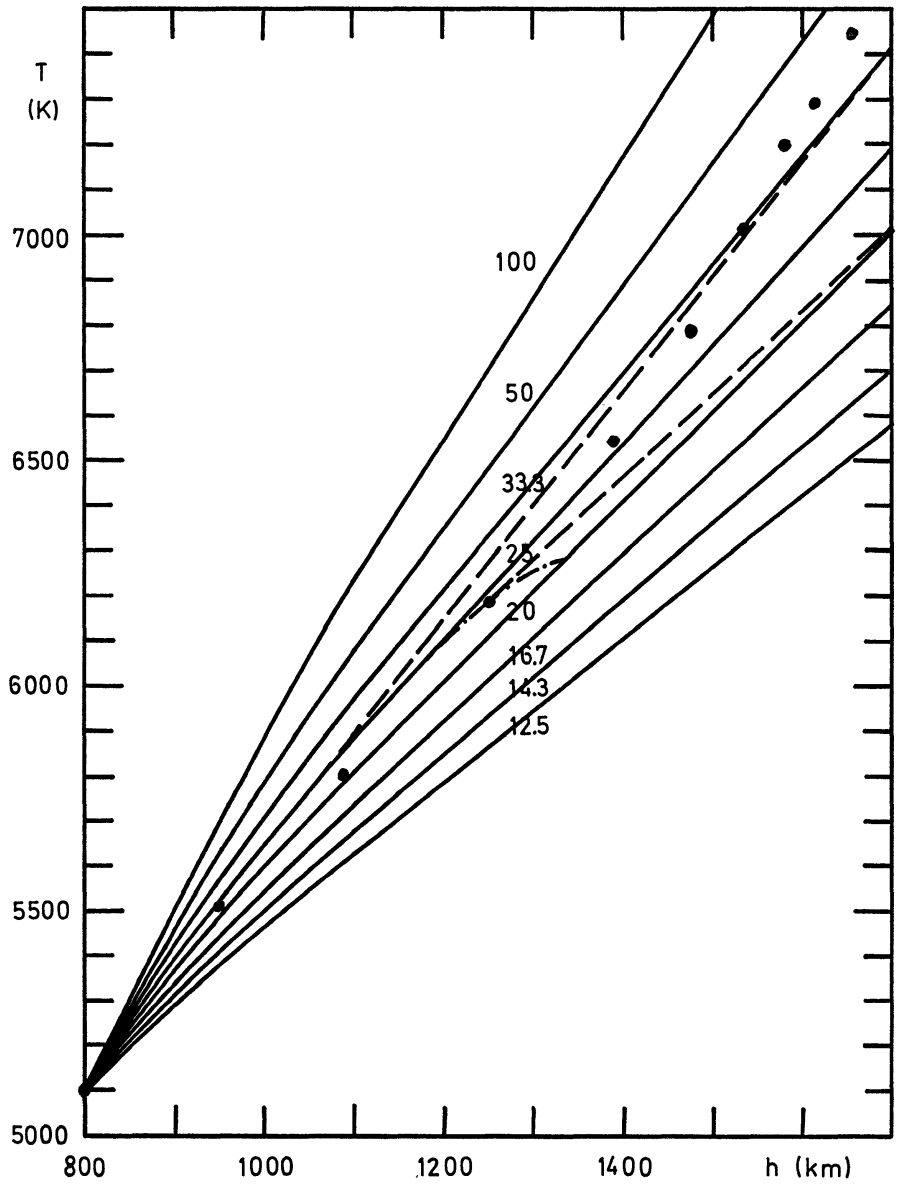

FIG. 18
Temperature T versus height h for theoretical chromospheric models of the Sun with the shock wave period as free parameter. Values indicate periods in s. Dots give the observational model of NOYES and KALKOFEN (1970).

In fig. 18 theoretical chromospheric models are shown which start from a boundary point of $T_0 = 5100\,°\mathrm{K}$, $p_0 = 100$ dyn/cm^2 at $x_0 = 800$ km with different periods P. This boundary point was taken from an empirical model. Note that the choice of T_0 and P fixes the value $F_{M\bullet}$ through eq. (100). Because eq. (99) is only valid for a fully developed sawtooth shock the height was chosen considerably above the temperature minimum in order to ensure that the shock is developed fully (see ULMSCHNEIDER 1971b, figs 4, 5). It is interesting that agreement between theoretical and empirical models is found for short period waves with periods between 20 to 25 s.

13 - Shocks of arbitrary strength, time dependent shock heating

The width of a shock is generally in the order of an atomic mean free path (LANDAU and LIFSHITZ 1959, p. 340). The mean free path l is given by

$$l = \frac{v\,t}{N\,q\,v\,t} = \frac{1}{N\,q} \approx \frac{1}{N\,\pi\,a_0^2} \approx \frac{10^{16}}{N}. \tag{102}$$

Here a_0 is the Bohr radius and N the number density. For $N = 10^{17}$ cm^{-3} at $a = 0$ km to $N = 10^{12}$ cm^{-3} at $x = 2000$ km from the photosphere to the top of the chromosphere l varies between 0.1 cm and 10 m. These distances are very small against characteristic geometric distances like the wavelength or the scale height. Moreover the optical distance across the width of the shock is less than 10^{-9}. Thus the shock can be treated as a discontinuity. If region 1 and 2 define the front and back of the shock, velocities relative to the shock at rest are given by

$$v_1 = u_1 - U_{SH} \tag{103}$$

$$v_2 = u_2 - U_{SH} \tag{104}$$

where U_{SH} is the velocity of the shock in the Euler (Laboratory) frame. As mass flux, momentum flux and energy flux must be continuous across a discontinuity we have the Hugoniot relations (LANDAU and LIFSHITZ, 1959, p. 319)

$$\rho_1 V_1 = \rho_2 V_2 \tag{105}$$

$$p_1 + \rho_1 V_1^2 = p_2 + \rho_2 V_2^2 \tag{106}$$

$$\frac{1}{2} V_1^2 + \frac{\gamma}{\gamma - 1} \frac{R}{\mu} T_1 = \frac{1}{2} V_2^2 + \frac{\gamma}{\gamma - 1} \frac{R}{\mu} T_2 . \tag{107}$$

Eq. (107) is valid for a neutral gas, as is the case in the photosphere and chromosphere. Note that at a discontinuity no radiation terms appear in eq. (107).

Eliminating p, ρ and T from eqs (106), (107) using eqs (11), (65) we find

$$U_{SH} = u_1 + \frac{\gamma+1}{4}(u_2 - u_1) + \left[\left(\frac{\gamma+1}{4}\right)^2 (u_2 - u_1)^2 + c_1^2\right]^{1/2} \tag{108}$$

$$c_2 = \left[\frac{\gamma-1}{2}(V_1^2 - V_2^2) + c_1^2\right]^{1/2} \tag{109}$$

$$S_2 = S_1 + \frac{2}{\gamma-1}\frac{R}{\mu} ln \frac{c_2}{c_1} - \frac{R}{\mu} ln \frac{V_1}{V_2}. \tag{110}$$

Defining the shock strength

$$\eta = \frac{\rho_2 - \rho_1}{\rho_1} \tag{111}$$

one can show using eqs (105) to (107) and (11) that

$$e^{\frac{(S_2-S_1)(\gamma-1)\mu}{R}} = \left(\frac{c_2}{c_1}\right)^2 \left(\frac{\rho_1}{\rho_2}\right)^{\gamma-1} = \frac{1 + \frac{\gamma-1}{2}\eta}{\left(1 - \frac{\gamma-1}{2}\eta\right)(1+\eta)^\gamma} \tag{112}$$

and

$$V_2 - V_1 = c_1 \eta \left(1 - \frac{\gamma-3}{2}\eta - \frac{\gamma-1}{2}\eta^2\right)^{-1/2} \equiv 2u_0. \tag{113}$$

Expanding these equations for *weak shocks* $\eta \ll 1$ we have

$$S_2 - S_1 \approx \frac{R}{\mu}\frac{\gamma(\gamma+1)}{12}\eta^3. \tag{114}$$

Using eq. (114) and eliminating η with eq. (113) we find

$$\frac{dF_M}{dx} \approx -\frac{\rho_0 T_0 (S_2 - S_1)}{P} \approx -\rho_0 \frac{2(\gamma+1)}{3}\frac{u_0^3}{c_0 P} \tag{115}$$

which with eq. (92) is identical to eq. (95).

With the modified method of characteristics the computation of the state near a *shock of arbitrary amplitude* is shown in fig. 19.

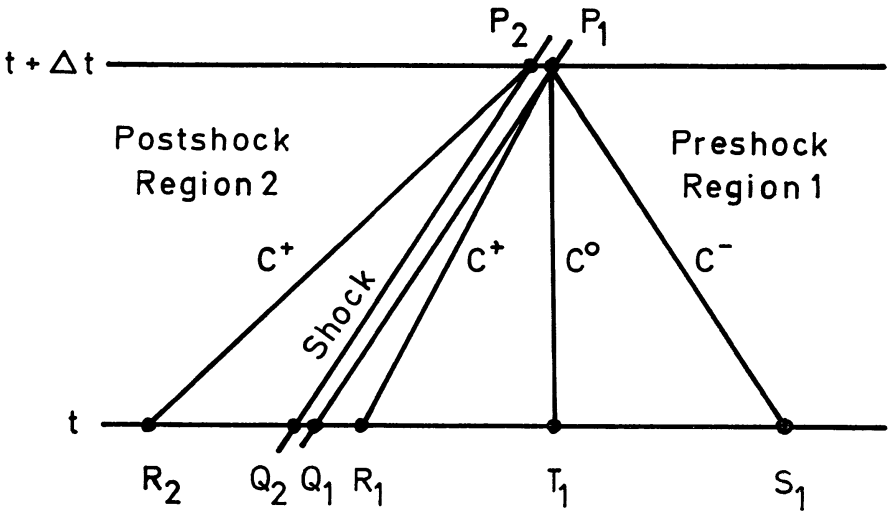

FIG. 19
Computation of the solution at a shock point P_1, P_2.

We assume the solution to be given at the time t. The shock occurs between two infinitesimally distant points Q_1, Q_2. At time $t + \Delta t$ the physical state at P_1, P_2 is determined by the four characteristics emanating from these points and intersecting the time level t at points R_2, R_1, T_1, S_1. Note that the shock is supersonic with respect to region 1, overtaking the C^+ characteristic there, and subsonic with respect to region 2. The seven unknowns u_1, c_1, S_1, u_2, c_2, S_2 and a_P, the latter being the position of the shock at the new time, are determined by the four differential eqs (63), (63), (66), (68) along the four characteristics, and the three Hugoniot relations (108) to (110), where eq. (108) has to be converted to the Lagrange frame using eq. (49). With this procedure the correct entropy jump $S_2 - S_1$ and the heating are evaluated automatically.

14 - Comparison of chromospheric heating mechanisms

In this section we want to compare the short period acoustic heating theory with possible other heating mechanisms. One presently (ULMSCHNEIDER 1974) thinks of three further heating mechanisms: gravity waves, 300 s oscillations, Alfven waves and magnetic field annihilation.

a) *Short period acoustic waves*

The following points are in favour of the short period acoustic heating theory.

1) Short period waves of large flux are observed (DEUBNER 1975, 1976).

2) Short period waves with an acoustic spectrum peaking at periods near 30 s are predicted theoretically (STEIN 1968, and Section 10).

3) Short period waves are able to explain the empirical height of the temperature minimum in the Sun and some stars (Section 10, figs 13, 14 and Table 1).

4) Short period waves have the right energy flux in order to explain the total empirical chromospheric emission (Section 10, figs 15, 16 and Table 1).

5) Short period waves explain the empirical gradient of emission in the chromosphere.

The last point is seen considering fig. 20.

In fig. 20 the empirical emission rate of the chromosphere as a function of height is shown as well as the rate of dissipation of acoustic shock waves of various energy fluxes and periods. The emission is computed using an empirical model and eq. (101). The dissipation is found integrating eq. (99). It is seen, in agreement with the conclusion drawn in Section 12 (fig. 18), that the shock waves need

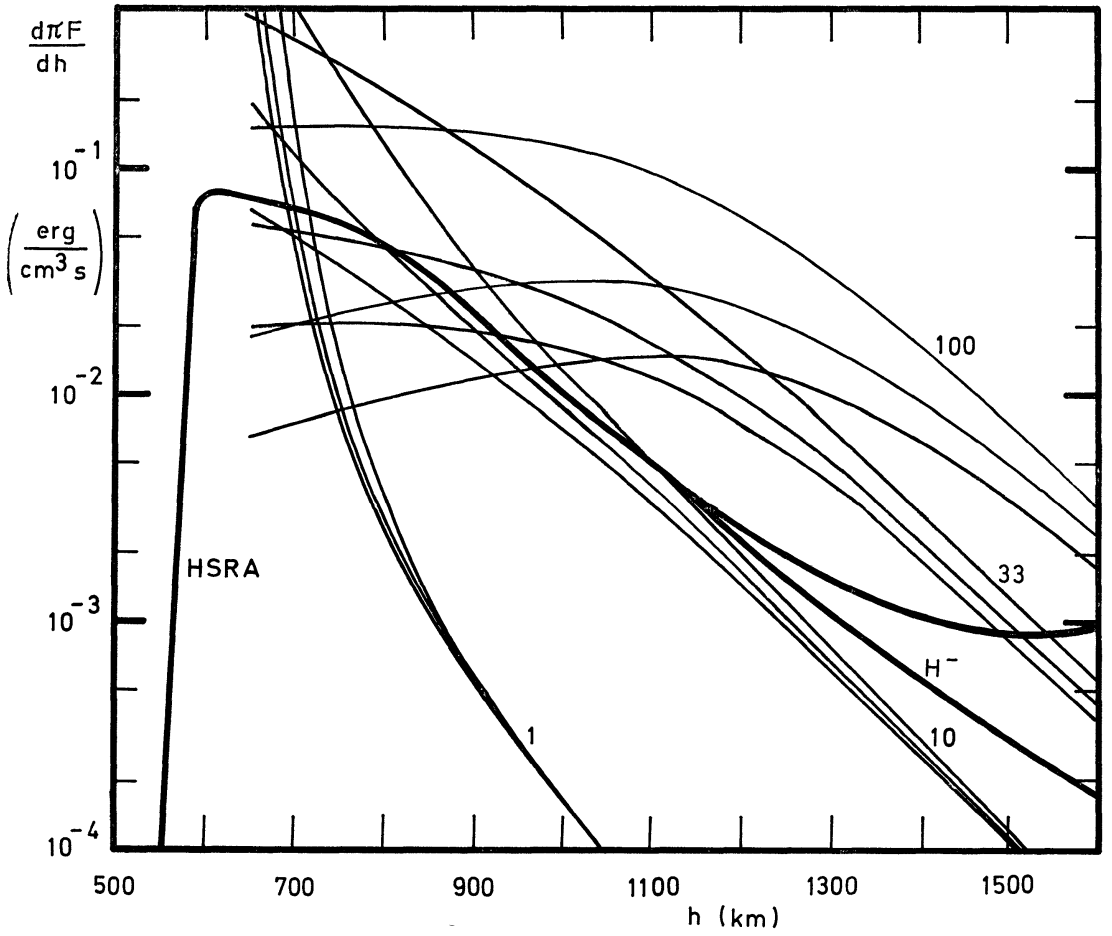

FIG. 20
Radiation loss rates (heavy lines) compared with shock dissipation rates (thin lines) in the HSRA. The shock dissipation curve families are labeled by the wave periods in s and have initial fluxes 1.0 E6, 4.0 E6, 8.0 E6 erg $cm^{-2} s^{-1}$, bottom to top.

to have short periods in order to explain the rapid decrease of chromospheric emission.

A difficulty for the short period acoustic heating theory is the observed fact that the chromospheric emission is with greater altitude increasingly concentrated in the chromospheric network. Here an enhanced generation of acoustic waves in the presence of magnetic fields (KULSRUD 1955), a delay of shock formation by the magnetic field resulting in a greater shock energy at larger altitudes (UCHIDA 1963) or some mechanism transfering acoustic energy into magnetic regions may provide an explanation.

b) *Gravity waves*

These waves (STEIN and LEIBACHER 1974) have not been observed on the Sun. The reason for this may be that they are not allowed to propagate in the convection zone and should suffer severe radiative damping at optical depths $\tau = 10$ to .01. At greater heights overshooting granulation could excite gravity waves. Both the height of the temperature minimum, because of their large periods and the chromospheric energy requirement can not be explained by gravity waves.

c) *300 second oscillations*

These waves (STEIN and LEIBACHER 1974) represent overstable nonradial evanescent acoustic modes of pulsation of the Sun (see e.g. DEUBNER 1975, ANDO and OSAKI 1975). From their evanescent nature and a more detailed investigation (CANFIELD and MUSMAN 1973, ZHUGHSDA 1973, ULMSCHNEIDER 1976) it appears that these waves do not transport enough energy to explain the chromospheric emission. These waves due to their long periods do not explain the height of the temperature minimum. Because shock dissipation, as opposed to radiative, conductive and viscous heating, is the dominant heating mechanism in the chromosphere, 300 s oscillations must be unimportant because of the observed 90° phase shift between velocity and temperature oscillation (DEUBNER 1974). In a shock wave this phase shift is zero (see fig. 21).

d) *Alfvén waves*

Alfvén waves (PIDDINGTON 1973, 1976; UCHIDA and KABURAKI 1974) are very likely not a significant chromospheric heating mechanism. A recent estimate of the energy flux of Alfvén waves (PIDDINGTON 1976) on basis of horizontal granular motion seems to be much too large. Granular flow, due to the with height increasing Alfvén speed, very likely gives rise not to Alfvén waves, but simply to a secular change of the magnetic field configuration (SCHMIDT 1976). Even under the assumption that Alfvén waves of sufficient energy are present it is difficult to explain how such waves should dissipate in a medium where the Alfvén speed is increasing thus decreasing dissipation rate with height, which is opposed to the observed strong dissipation starting at heights above the temperature minimum and being essentially zero below.

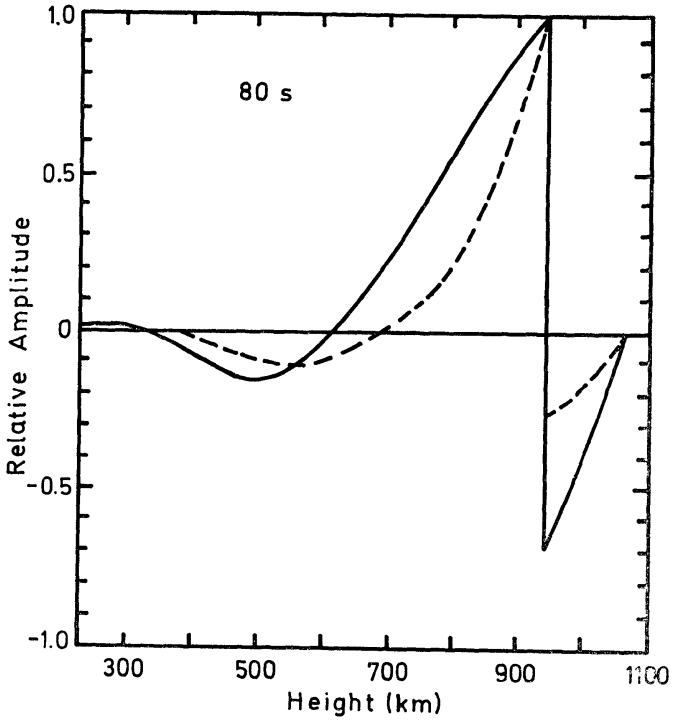

FIG. 21
Shock wave of 80 s period in a gravitational atmosphere. The velocity perturbation is shown drawn, the temperature perturbation is shown dashed.

e) *Magnetic field annihilation*

This mechanism proposed by John Leibacher at this Erice School is little understood.

f) *Heating mechanisms for the corona*

Coronal heating is presently not well understood. Here heating mechanisms which are unimportant in the chromosphere like the 300 s oscillations or Alfvén waves may well become dominant and be competitive or replace the acoustic heating.

Literature

ANDO, H. and OSAKI, Y. 1975, *Publ. Astron. Soc. Japan*, **27**, 581.
AYRES, T. R. 1975, *Ph. D. Thesis*, Univ. of Colorado, Boulder.
BRAY, R. J. and LOUGHHEAD, R. E. 1974, *The Solar Chromosphere*, Chapman and Hall, London.
CANFIELD, R. C. and MUSMAN, S. 1973, *Ap. J.*, **184**, L 131.
CHRISTENSEN-DALSGAARD, J. and GOUGH, D. O. 1976, *Nature*, **259**, 89.
DEUBNER, F. 1974, *Solar Phys.*, **39**, 31.
DEUBNER, F. 1975, *Nice meeting on Physics of Motions in Stellar Atmospheres*, International Colloquium of the CNRS, R. Cayrel and M. Steinberg Eds., 1976.
DEUBNER, F. 1976, *Astron. Astrophys.*, **51**, 189.

ECKART, C. 1960, *Hydrodynamics of Oceans and Atmospheres*, Pergamon Press, Oxford.
GINGERICH, O., NOYES, R. W., KALKOFEN, W. and CUNY, Y. 1971, *Solar Phys.*, **18**, 347.
HOSKIN, N. E. 1964, *Meth. Comp. Phys.*, **3**, 265.
KALKOFEN, W. and ULMSCHNEIDER, P. 1976, *Astron. Astrophys.*, to be published.
KULSRUD, R. M. 1955, *Ap. J.*, **121**, 461.
KUPERUS, M. 1965, *Rech. Astron. Observ. Utrecht*, **17**, 1.
KURUCZ, R. 1970, *SAO Spec. Report.*, **309**.
LANDAU, L. D. and LIFSHITZ, E. M. 1959, *Fluid Mechanics*, Pergamon Press, London.
LISTER, M. 1960, in *Math. Methods for Digital Computers* I, Ralston A. and Wilf H. S. Eds., Wiley, New York.
MCWHIRTER, R. W. P., THONEMANN, P. C. and WILSON, R. 1975, *Astron. Astrophys.*, **40**, 63.
MIHALAS, D. 1971, *Stellar Atmospheres*, Freeman, San Francisco.
NOYES, R. W. and KALKOFEN, W. 1970, *Solar Phys.*, **15**, 120.
PIDDINGTON, J. H. 1973, *Solar Phys.*, **33**, 363.
PIDDINGTON, J. H. 1976, *Astrophys. Space Sci.*, **41**, 371.
SCHMIDT, H. U. 1976, private communication.
STEIN, R. F. 1968, *Ap. J.*, **154**, 297.
STEIN, R. F. and LEIBACHER, J. 1974, *Ann. Rev. Astron. Astrophys.*, **12**, 407.
UCHIDA, Y. 1963, *Publ. Astron. Soc. Japan*, **15**, 376.
UCHIDA, Y. and KABURAKI, O. 1974, *Solar Phys.*, **35**, 451.
ULMSCHNEIDER, P. 1971a, *Astron. Astrophys.*, **12**, 297.
ULMSCHNEIDER, P. 1971b, *Astron. Astrophys.*, **14**, 275.
ULMSCHNEIDER, P. 1974, *Solar Phys.*, **39**, 327.
ULMSCHNEIDER, P. 1976, *Solar Phys.*, in press.
ULMSCHNEIDER, P., KALKOFEN, W., NOWAK, T. and BOHN, H. U. 1976, *Astron. Astrophys.*, in press.
VANBEVEREN, D. and DE LOORE, C. 1976, to be published.
ZELDOVICH, Y. B. and RAIZER, YU. P. 1966, *Physics of Shock Waves and High-Temperature Hydrodynamic Phenomena*, Academic Press, New York.
ZHUGHSDA, YU. D. 1973, *Astrophys. Letters*, **13**, 173.